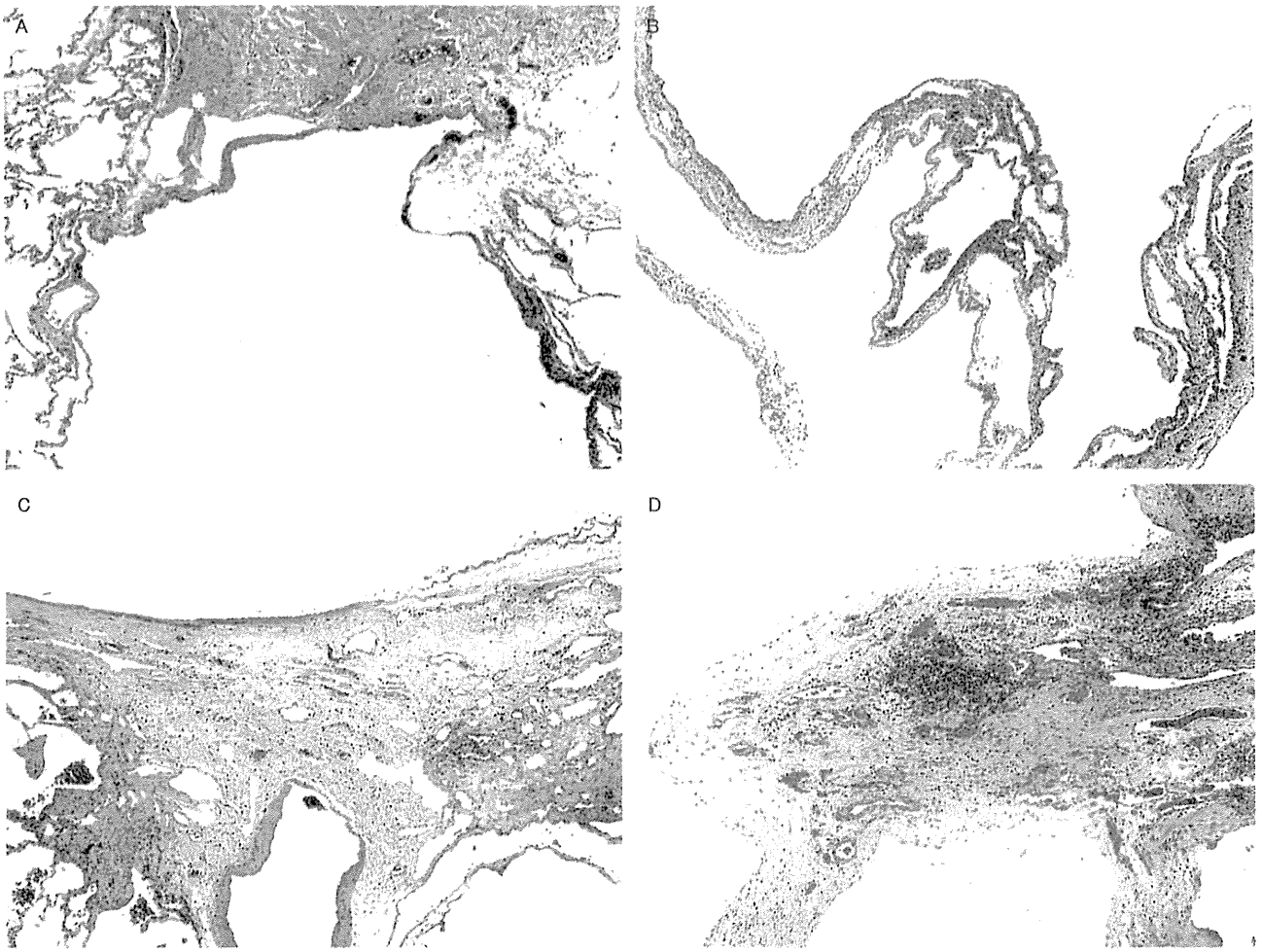

Figure 2. Representative photomicrographs showing cyst-associated cellular and/or fibrous inflammation: A, no inflammation (from an intrapulmonary cyst in Birt–Hogg–Dubé syndrome, BHDS: note that the cyst abuts on an interlobular septum in the upper area); B, cellular inflammation (from a subpleural cyst in BHDS); C, fibrous inflammation (from bullae in primary spontaneous pneumothorax, PSP); and D, cellular and fibrous inflammation (from bullae in PSP).

MORPHOMETRIC ANALYSIS

We examined the histological features of cysts in terms of size and location in the lung parenchyma. The maximum diameter of cysts associated with BHDS ranged from 1.0 to 15.7 mm (median: 3.8 mm), and two-thirds of them had diameters of ≤5 mm. A histogram depicting our analysis of size shows that the number of the cysts logarithmically diminished as the maximum cyst size increased [correlation coefficient for the fitted curve, $y = -23.3 \ln(x) + 63.0$, $R^2 = 0.925$] (Figure 3). In addition, the proportion of cysts with inflammation increased as the maximum cyst size increased. However, no significant difference was noted in maximal cyst size between men and women [median 4.0 mm (range 1–15.7 mm) versus 3.5 mm (range 1.0–13.2 mm), $P = 0.6908$] or between patients with or without a history of smoking [median 4.0 mm (range 1.0–12.6 mm) versus 3.4 mm (range 1.0–15.7), $P = 0.1508$]. Statistical significance was evident for the larger size of subpleural cysts than of intrapulmonary cysts [median 5.0 mm (range 1.0–15.7 mm) versus 3.0 mm (range 1.0–9.8 mm), $P < 0.0001$] and for the larger size of cysts with inflammation than of those without inflammation [median 4.7 mm (range 1.1–15.7 mm) versus 3.3 mm (range 1.0–9.8 mm), $P < 0.0001$]. When we evaluated the influence of location or inflammation on maximum cyst size, the results demonstrated that subpleural cysts with inflammation were significantly larger than those without inflammation. However, the size of in-

Table 3. Comparison of the numbers of subpleural cysts with inflammation in Birt–Hogg–Dubé syndrome (BHDS) and primary spontaneous pneumothorax (PSP). Inflammation was examined with regard to the location of the cyst (pleural or basal site) and type of inflammation (cellular or fibrous)

	No. of subpleural cysts examined	No. of cysts with inflammation (%)	Inflammation at pleural site, no. (%)		Inflammation at basal site, no. (%)	
			Cellular	Fibrous	Cellular	Fibrous
BHDS	116	79 (68.1)	75 (64.7)	55 (47.4)	19 (16.4)	6 (5.2)
PSP	115	115 (100)	73 (63.5)	115 (100)	56 (48.7)	106 (92.2)
χ^2–test		$P < 0.001$	$P = 0.852$	$P < 0.001$	$P < 0.001$	$P < 0.001$

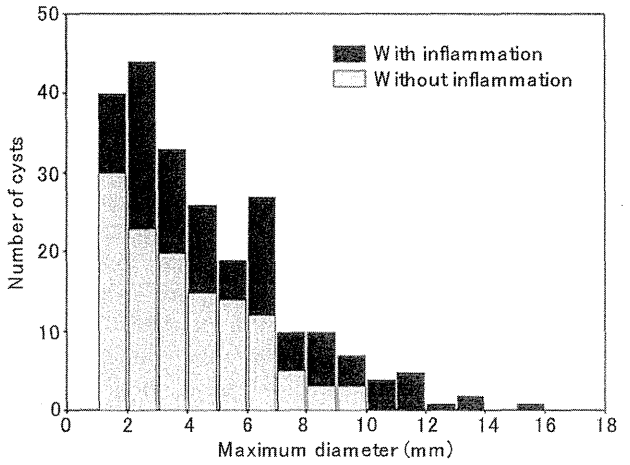

Figure 3. Distribution of the maximum diameter of pulmonary cysts in patients with Birt–Hogg–Dubé syndrome. Black and grey columns indicate the numbers of pulmonary cysts with and without inflammation, respectively.

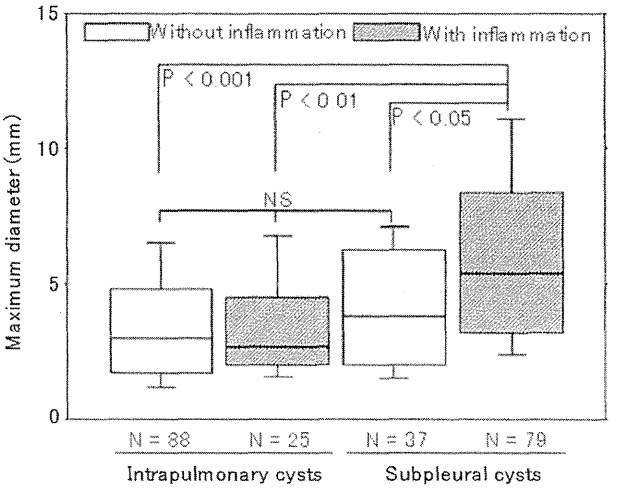

Figure 4. Comparison of the maximum diameters of intrapulmonary and subpleural cysts in patients with BHDS.

trapulmonary cysts was not affected by the presence or absence of inflammation, and the size of subpleural cysts without inflammation resembled that of non-inflamed intrapulmonary cysts (Figure 4).

Discussion

We have demonstrated the unique histological characteristics of pulmonary cysts from 50 unrelated patients with BHDS, the largest cohort ever included in a study of lung pathology focusing on BDHS. Our results show that pulmonary BHDS cysts are: (i) surrounded by normal alveolar walls; (ii) abut on interlobular septa; and (ii) may have intracystic septa and/or protrusion of venules into the cystic space, indicating disappearance of the surrounding alveolar wall and/or regression of connective tissue of interlobular septa. These histological characteristics can differentiate BHDS from other cystic lung diseases. For example, tuberous sclerosis complex (TSC)-associated lymphangioleiomyomatosis (LAM) always shows LAM cell proliferation in the cyst walls. In other hereditary cystic lung diseases, such as cystic fibrosis, Ehlers–Danlos syndrome, and Marfan syndrome, patients have non-specific cystic lesions with cellular or fibrous inflammation.[22–24] In the non-hereditary lung cystic diseases, including Langerhans cell histiocytosis, amyloidosis, Sjögren syndrome, and lymphocytic interstitial pneumonia, infiltration of inflammatory cells and/or matrix deposition always occurs.[25]

The present study clearly establishes that neither inflammation nor cell proliferation contributes to cyst formation in patients with BHDS, because most of their cysts, especially intrapulmonary BHDS cysts that do not suffer from the secondary effects of pneumothorax, show neither inflammation nor abnormal cell proliferation. As the majority of BHDS cysts are

located far from bronchioles, the mechanism for cyst formation in BHDS is less likely to be associated with a check-valve mechanism, which is supposedly operative on cyst formation in PSP, smoking-related diseases, Sjögren syndrome, and other non-hereditary cystic lung diseases. We have demonstrated in the present study that most of the intrapulmonary BHDS cysts (88/113, 77.9%) lack inflammation, whereas only approximately one-third of the subpleural cysts (37/116, 31.9%) have no inflammation (Table 2). Accordingly, we think that most, if not all, of the inflammatory changes observed were associated with pneumothorax. It has already been well described that pneumothorax causes pleural inflammation at the pleural side of the cyst, but not at the basal side.[26] In addition, an animal experiment clearly showed that repeated injection of air into the pleural space caused inflammation and the formation of 'neomembranes' composed of fibroblasts and collagen that was variably covered by proliferation of mesothelial cells.[27] In addition, the finding that the BHDS cysts without inflammation had no significant difference in size, irrespective of whether they were subpleural or intrapulmonary (Figure 4), suggests that inflammation secondary to pneumothorax is likely to contribute to the subsequent growth of subpleural cysts in BHDS. Interestingly, we have demonstrated a logarithmic decline in the number of cysts as the size of individual cysts increases. Possibly, the fusion of small cysts resulted in the enlargement that we noted. This process may also explain how intracystic septa develop in BHDS cysts, as abutting cysts could fuse with intervening interlobular septa. In this context, the protrusion of venules into ~40% of the BHDS cysts may have been caused not only by the disappearance of alveolar walls adjoining interlobular septa, but also by regression of their surrounding connective tissue in the septa.

The mechanism for development of pulmonary cysts in BHDS has been discussed in several reports. Graham *et al.*[14] speculated that a genetic abnormality was responsible for postnatal alveolar proliferation of the peripheral lung, on the basis of pathological examination of three BHDS non-smokers, as they found cysts predominantly in the subpleural area. Warren *et al.*[28] found that *FLCN* was expressed in type I pneumocytes and stromal cells, including fibroblasts and macrophages in the lungs, and hence proposed a possible role for functional abnormalities of these folliculin-expressing cells in cyst formation. Recently, Furuya *et al.*[4] reported that dysregulation of the mTOR pathway resulting from haploinsufficiency of *FLCN* may induce cyst formation through proliferation of type II pneumocytes. However, the above mechanisms were deduced from an examination of limited numbers of lung specimens, and are therefore unlikely to fit the histopathological features of BHDS cysts and lungs defined after detailed analysis of the much larger specimen sample presented here. For example, cysts are present not only in subpleural areas but also in parenchyma, and most cysts have neither cellular proliferation nor inflammation, especially cysts in the parenchymal area, where secondary changes resulting from pneumothorax would not affect the pathological findings, in contrast to cysts at subpleural sites. In addition, when bullae/blebs are affected by pneumothorax, they will usually have reactive proliferation of type II pneumocytes. If proliferation of type II pneumocytes were actively involved in cyst formation, those cysts would show no predilection for the location and distribution recorded here; instead, they should be detectable not only in the area surrounded by interlobular septa, but also in the centrilobular area. Furthermore, one would expect cyst formation to proceed by proteolysis, as in smoke-related inflammatory diseases, collagen diseases, and neoplastic diseases such as LAM.[29] Otherwise, the proliferation of type II pneumocytes might form a lung tumour, like multifocal micronodular pneumocyte hyperplasia occurring via dysregulation of the mTOR pathway in patients with TSC.[18] However, in the present study, lung specimens from BHDS patients showed no destruction of lung architecture by either proliferating type II pneumocytes or inflammation, indicating that BHDS cysts may not develop through proliferation of type II pneumocytes or proteolysis mediated by proliferating type II pneumocytes.

Presumably, considering the unique histological characteristics of BHDS cysts defined by the present study, almost all cysts abutting on interlobular septa without significant inflammation should ensue naturally from the inherent mechanism of cyst formation. In this context, we postulate that *FLCN* mutation results in abnormalities at the alveolar-septal junction. Several reports have described folliculin, the protein encoded by *FLCN*, as a regulator of TGF-β signalling, especially TGF-β_2,[30] or cell–cell adhesion through the interaction with adherence junction protein.[31] TGF-β_2 is involved in epithelial–mesenchymal interactions, cell growth, the production of extracellular matrix proteins, and tissue remodelling during development or normal subepithelial matrix homeostasis.[32,33] Warren *et al.*[28] demonstrated that *FLCN* mRNA was strongly expressed in stromal cells within the connective tissue and weakly in type I

pneumocytes in the lung. This topographic expression pattern indicates that folliculin may participate in maintaining the homeostasis of alveolar walls through effects on stromal cells and/or type I pneumocytes. We recently found that lung fibroblasts isolated from patients with BHDS showed diminished migration as well as decreased expression of TGF-β and extracellular matrix proteins (manuscript in preparation). These findings imply that the alveolar-septal junction may become vulnerable to mechanical forces throughout the entire alveolar wall meshwork during respiratory cycles of inflation and deflation, leading to cyst formation resulting from the disruption of alveolar homeostasis. Supporting this notion is the fact that the periacinar regions where alveoli attach to connective tissue septa are weak from an anatomical as well as a physiological viewpoint. Capillaries in alveolar walls abutting on connective tissue septa or visceral pleura are less numerous than elsewhere, and the periacinar regions then have less vascularity and greater compliance.[34] Furthermore, our hypothesis based on histopathological study seems to be well formulated to explain the results of our previous radiological study, showing that BHDS cysts are irregularly shaped rather than oval, and are predominantly located in the lower medial lung zone:[35] (i) a cyst's periacinar development would contribute to its irregular shape, caused by imbalanced elastic recoil forces of the remaining alveolar tissues within a unit structure of a secondary lobule;[36] and (ii) greater mechanical force would be loaded onto the lower lobes than onto the upper lobes during respiratory cycles. However, further studies are needed to confirm this hypothesis.

In conclusion, we have defined the unique histological features of pulmonary cysts in patients with BHDS, almost all cysts abutting on interlobular septa without significant inflammation. The 229 BHDS cysts derived from lung specimens of 50 unrelated patients surveyed here constitute the most extensive of such studies.

Acknowledgements

The authors greatly thank Dr Hitoshi Niino, Division of Clinical Laboratory, National Hospital Organization Yokohama Medical Centre, Kanagawa, Japan, for providing the macroscopic figures of lung tissue, and Dr Noriyo Yanagawa, Department of Radiology, Tsukuba Memorial Hospital, Tochigi, Japan, for fruitful discussion. We also thank Ms Phyllis Minick for her excellent proofreading of our English.

References

1. Schmidt LS, Nickerson ML, Warren MB *et al.* Germline BHD-mutation spectrum and phenotype analysis of a large cohort of families with Birt–Hogg–Dube syndrome. *Am. J. Hum. Genet.* 2005; **76**; 1023–1033.
2. Nickerson ML, Warren MB, Toro JR *et al.* Mutations in a novel gene lead to kidney tumors, lung wall defects, and benign tumors of the hair follicle in patients with the Birt–Hogg–Dube syndrome. *Cancer Cell* 2002; **2**; 157–164.
3. Baba M, Hong SB, Sharma N *et al.* Folliculin encoded by the BHD gene interacts with a binding protein, FNIP1, and AMPK, and is involved in AMPK and mTOR signaling. *Proc. Natl Acad. Sci. USA* 2006; **103**; 15552–15557.
4. Furuya M, Tanaka R, Koga S *et al.* Pulmonary cysts of Birt–Hogg–Dube syndrome: a clinicopathologic and immunohistochemical study of 9 families. *Am. J. Surg. Pathol.* 2012; **36**; 589–600.
5. Hartman TR, Nicolas E, Klein-Szanto A *et al.* The role of the Birt–Hogg–Dube protein in mTOR activation and renal tumorigenesis. *Oncogene* 2009; **28**; 1594–1604.
6. Hasumi H, Baba M, Hong SB *et al.* Identification and characterization of a novel folliculin-interacting protein FNIP2. *Gene* 2008; **415**; 60–67.
7. Linehan WM, Bratslavsky G, Pinto PA *et al.* Molecular diagnosis and therapy of kidney cancer. *Annu. Rev. Med.* 2010; **61**; 329–343.
8. Takagi Y, Kobayashi T, Shiono M *et al.* Interaction of folliculin (Birt–Hogg–Dube gene product) with a novel Fnip1-like (FnipL/Fnip2) protein. *Oncogene* 2008; **27**; 5339–5347.
9. Toro JR, Wei MH, Glenn GM *et al.* BHD mutations, clinical and molecular genetic investigations of Birt–Hogg–Dube syndrome: a new series of 50 families and a review of published reports. *J. Med. Genet.* 2008; **45**; 321–331.
10. Vocke CD, Yang Y, Pavlovich CP *et al.* High frequency of somatic frameshift BHD gene mutations in Birt–Hogg–Dube-associated renal tumors. *J. Natl Cancer Inst.* 2005; **97**; 931–935.
11. van Steensel MA, Verstraeten VL, Frank J *et al.* Novel mutations in the BHD gene and absence of loss of heterozygosity in fibrofolliculomas of Birt–Hogg–Dube patients. *J. Invest. Dermatol.* 2007; **127**; 588–593.
12. Furuya M, Nakatani Y. Birt–Hogg–Dube syndrome: clinicopathological features of the lung. *J. Clin. Pathol.* 2013; **66**; 178–186.
13. Ayo DS, Aughenbaugh GL, Yi ES, Hand JL, Ryu JH. Cystic lung disease in Birt–Hogg–Dube syndrome. *Chest* 2007; **132**; 679–684.
14. Graham RB, Nolasco M, Peterlin B, Garcia CK. Nonsense mutations in folliculin presenting as isolated familial spontaneous pneumothorax in adults. *Am. J. Respir. Crit. Care Med.* 2005; **172**; 39–44.
15. Ishii H, Oka H, Amemiya Y *et al.* A Japanese family with multiple lung cysts and recurrent pneumothorax: a possibility of Birt–Hogg–Dube syndrome. *Intern. Med.* 2009; **48**; 1413–1417.
16. Koga S, Furuya M, Takahashi Y *et al.* Lung cysts in Birt–Hogg–Dube syndrome: histopathological characteristics and aberrant sequence repeats. *Pathol. Int.* 2009; **59**; 720–728.
17. Butnor KJ, Guinee DG Jr. Pleuropulmonary pathology of Birt–Hogg–Dube syndrome. *Am. J. Surg. Pathol.* 2006; **30**; 395–399.
18. Hayashi M, Takayanagi N, Ishiguro T, Sugita Y, Kawabata Y, Fukuda Y. Birt–Hogg–Dube syndrome with multiple cysts and

recurrent pneumothorax: pathological findings. *Intern. Med.* 2010; **49**; 2137–2142.
19. Gunji Y, Akiyoshi T, Sato T *et al.* Mutations of the Birt Hogg Dube gene in patients with multiple lung cysts and recurrent pneumothorax. *J. Med. Genet.* 2007; **44**; 588–593.
20. Kunogi M, Kurihara M, Ikegami TS *et al.* Clinical and genetic spectrum of Birt–Hogg–Dube syndrome patients in whom pneumothorax and/or multiple lung cysts are the presenting feature. *J. Med. Genet.* 2010; **47**; 281–287.
21. Hammar SP. Pneumothorax. In Tomashefski JF Jr, Cagle PT, Farver C, Fraire AE eds. *Dail and Hammar's pulmonary pathology, Vol. 1*: Nonneoplastic lung disease, 3rd ed. New York: Springer Science/Business Media, LLC, 2008; 1167–1168.
22. Tomashefski JF Jr, Bruce M, Stern RC, Dearborn DG, Dahms B. Pulmonary air cysts in cystic fibrosis: relation of pathologic features to radiologic findings and history of pneumothorax. *Hum. Pathol.* 1985; **16**; 253–261.
23. Kawabata Y, Watanabe A, Yamaguchi S *et al.* Pleuropulmonary pathology of vascular Ehlers-Danlos syndrome: spontaneous laceration, haematoma and fibrous nodules. *Histopathology* 2010; **56**; 944–950.
24. Dyhdalo K, Farver C. Pulmonary histologic changes in Marfan syndrome: a case series and literature review. *Am. J. Clin. Pathol.* 2011; **136**; 857–863.
25. Seaman DM, Meyer CA, Gilman MD, McCormack FX. Diffuse cystic lung disease at high-resolution CT. *AJR Am. J. Roentgenol.* 2011; **196**; 1305–1311.
26. Lichter I, Gwynne JF. Spontaneous pneumothorax in young subjects. A clinical and pathological study. *Thorax* 1971; **26**; 409–417.
27. Churg AM. Pneumothorax. In Thurlbeck WM, Churg AM eds. *Pathology of the lung*, 2nd ed. New York, NY: Thieme Medical Publishers, 1995; 1078–1080.
28. Warren MB, Torres-Cabala CA, Turner ML *et al.* Expression of Birt–Hogg–Dube gene mRNA in normal and neoplastic human tissues. *Mod. Pathol.* 2004; **17**; 998–1011.
29. Colombat M, Caudroy S, Lagonotte E *et al.* Pathomechanisms of cyst formation in pulmonary light chain deposition disease. *Eur. Respir. J.* 2008; **32**; 1399–1403.
30. Hong SB, Oh H, Valera VA *et al.* Tumor suppressor FLCN inhibits tumorigenesis of a FLCN-null renal cancer cell line and regulates expression of key molecules in TGF-beta signaling. *Mol. Cancer* 2010; **9**; 160.
31. Medvetz DA, Khabibullin D, Hariharan V *et al.* Folliculin, the product of the Birt–Hogg–Dube tumor suppressor gene, interacts with the adherens junction protein p0071 to regulate cell–cell adhesion. *PLoS ONE* 2012; **7**; e47842.
32. Sanford LP, Ormsby I, Gittenberger-de Groot AC *et al.* TGFbeta2 knockout mice have multiple developmental defects that are non-overlapping with other TGFbeta knockout phenotypes. *Development* 1997; **124**; 2659–2670.
33. Thompson HG, Mih JD, Krasieva TB, Tromberg BJ, George SC. Epithelial-derived TGF-beta2 modulates basal and wound-healing subepithelial matrix homeostasis. *Am. J. Physiol. Lung Cell. Mol. Physiol.* 2006; **291**; L1277–L1285.
34. Fishman AP, Elias JA, Fishman JA, Grippi MA, Kaise LR, Senior RM. Bullous disease of the lung. In Fishman AP, Elias JA, Fishman JA, Grippi MA eds. *Fishman's pulmonary diseases and disorders*, 4th ed. New York, NY: McGraw-Hill, 2008; 913–929.
35. Tobino K, Gunji Y, Kurihara M *et al.* Characteristics of pulmonary cysts in Birt–Hogg–Dube syndrome: thin-section CT findings of the chest in 12 patients. *Eur. J. Radiol.* 2011; **77**; 403–409.
36. Morgan MD, Edwards CW, Morris J, Matthews HR. Origin and behaviour of emphysematous bullae. *Thorax* 1989; **44**; 533–538.

Ishii et al. BMC Pulmonary Medicine 2014, 14:37
http://www.biomedcentral.com/1471-2466/14/37

BMC
Pulmonary Medicine

RESEARCH ARTICLE Open Access

Secondary pulmonary alveolar proteinosis complicating myelodysplastic syndrome results in worsening of prognosis: a retrospective cohort study in Japan

Haruyuki Ishii[1], John F Seymour[2], Ryushi Tazawa[3], Yoshikazu Inoue[4], Naoyuki Uchida[5], Aya Nishida[5], Yoshihito Kogure[6], Takeshi Saraya[1], Keisuke Tomii[7], Toshinori Takada[8], Yuko Itoh[3], Masayuki Hojo[9], Toshio Ichiwata[10], Hajime Goto[1] and Koh Nakata[3*]

Abstract

Background: Secondary pulmonary alveolar proteinosis (sPAP) is a very rare lung disorder comprising approximately 10% of cases of acquired PAP. Hematological disorders are the most common underlying conditions of sPAP, of which 74% of cases demonstrate myelodysplastic syndrome (MDS). However, the impact of sPAP on the prognosis of underlying MDS remains unknown. The purpose of this study was to evaluate whether development of sPAP worsens the prognosis of MDS.

Methods: Thirty-one cases of sPAP and underlying MDS were retrospectively classified into mild and severe cases consisting of very low-/low-risk groups and intermediate-/high-/very high-risk groups at the time of diagnosis of MDS, according to the prognostic scoring system based on the World Health Organization classification. Next, we compared the characteristics, disease duration, cumulative survival, and prognostic factors of the groups.

Results: In contrast to previous reports on the prognosis of MDS, we found that the cumulative survival probability for mild MDS patients was similar to that in severe MDS patients. This is likely due to the poor prognosis of patients with mild MDS, whose 2-year survival rate was 46.2%. Notably, 75% and 62.5% of patients who died developed fatal infectious diseases and exacerbation of PAP, respectively, suggesting that the progression of PAP *per se* and/or PAP-associated infection contributed to poor prognosis. The use of corticosteroid therapy and a diffusing capacity of the lung for carbon monoxide of less than 44% were predictive of poor prognosis.

Conclusion: Development of sPAP during the course of MDS may be an important adverse risk factor in prognosis of patients with mild MDS.

Keywords: Proteinosis, Myelodysplastic syndrome, GM-CSF, WPSS, Secondary pulmonary alveolar proteinosis, MDS, PAP, Refractory anemia

* Correspondence: radical@med.niigata-u.ac.jp
[3]Bioscience Medical Research Center, Niigata University Medical & Dental Hospital, 1-754 Asahimachi-dori, Chuo-ku, Niigata 9518520, Japan
Full list of author information is available at the end of the article

Background

Pulmonary alveolar proteinosis (PAP), a rare disorder predominantly affecting the lungs, is characterized by accumulation of surfactant lipids and proteins in the alveoli and terminal bronchioles [1]. PAP is clinically classified into three distinct forms, namely, autoimmune, secondary, and congenital PAP [2]. Autoimmune PAP is associated with disruption of granulocyte/macrophage colony-stimulating factor (GM-CSF) signaling caused by high levels of GM-CSF autoantibody in the lungs [3]. Secondary PAP (sPAP) results from underlying diseases that presumably impair surfactant clearance because of abnormal numbers and functions of alveolar macrophages (AMs). Of the 40 cases of sPAP previously reported by our group [4], 88% (n = 35) involved hematological disorders as underlying diseases. The probability of survival at two years was 46% in cases with sPAP complicating hematological disorders. The median survival time for all cases including 17 patients who died within two years of the sPAP diagnosis was 16 months. Although myelodysplastic syndrome (MDS) is the most frequent underlying disease of sPAP (n = 26, 65%), little information is available on the prognostic impact of development of sPAP on patient outcome.

MDS, a group of clonal hematological stem-cell disorders with ineffective myeloid hematopoiesis and varying degrees of bone marrow failure, is associated with a significant risk of progression to acute myeloid leukemia (AML). Clinical manifestations are variable, from indolent conditions with near-normal life expectancy to forms that rapidly develop into AML [5]. Clarifying much of this heterogeneity, the World Health Organization (WHO) developed a classifications of MDS based on the presence of unilineage or multilineage dysplasia, bone marrow blast cell count, and cytogenetic features: refractory anemia (RA), RA with ringed sideroblasts (RARS), refractory cytopenia with multilineage dysplasia (RCMD), RCMD with ringed sideroblasts (RCMD-RS), RA with excess of blasts-1 (RAEB-1), and RA with excess of blasts-2 (RAEB-2) [6]. In 2007, Malcovati *et al.* developed a new prognostic scoring system (WHO classification-based prognostic scoring system (WPSS)) according to WHO subgroup, karyotype, and transfusion requirement. Through this system, cases with MDS are classified into very low-, low-, intermediate-, high-, or very high-risk groups [7]. WPSS is a dynamic system that accurately predicts the survival and risk of leukemic evolution in MDS patients at any time during the course of their disease. This time-dependent system seems particularly useful for lower-risk patients and for implementing risk-adapted treatment strategies.

Given the validation of WPSS criteria as a prognostic indicator for the course of MDS, it is applicable in prognosis evaluation of MDS complicated by PAP (MDS/sPAP). In the present study, we evaluated this issue for the first time and found that development of sPAP worsens the prognosis of patients with otherwise low-risk MDS.

Methods

Subjects

Thirty-one patients in Japan who were diagnosed with sPAP with underlying MDS from July 1999 to June 2013 were evaluated. We obtained agreement from all treating physicians for each identified case, according to the Guidelines for Epidemiological Studies by The Ministry of Health, Labour, and Welfare. This was a retrospective cohort study approved by the Ethical Board of Kyorin University (H23-085-01). Cases, part of which were reported previously, were identified retrospectively [8-18].

Diagnosis

Diagnosis of MDS was made according to the 2002 WHO criteria [6]. One patient with unclassified MDS, two patients with myelofibrosis, and two patients with 20% marrow blasts who were considered as having AML were excluded from the study. MDS with isolated chromosome 5 deletion (del(5q)) and marrow blasts of <5% were included. Next, the patients were classified into RA, RARS, RCMD, RAEB-1, and RAEB-2 groups. Karyotypes were classified by using the International System for Cytogenetic Nomenclature Criteria [19]. Diagnosis of PAP was based on the following criteria: 1. histopathological findings from specimens obtained by surgical biopsy or transbronchial lung biopsy, or milk-like appearance with typical cytological findings from bronchoalveolar lavage fluid (BALF); 2. typical high-resolution computed tomography (HRCT) findings for PAP, such as ground glass opacity, consolidation, and interlobular septal thickening; and 3. negative result for serum GM-CSF autoantibody.

Classification by WPSS

The WPSS score was calculated according to the method of Malcovati *et al.* [7] The score was calculated from the data of WHO subgroups (RA/RARS/5q−, RCMD/RCMD-RS, RAEB-1, and RAEB-2), karyotype abnormalities categorized according to the International Prognostic Scoring System [20], and transfusion requirement. The same weight (score of ≥1) was assigned to each variable for WHO subgroup, karyotype, and transfusion requirement. Based on the score, patients were classified according to the following five risk groups: very low (score = 0), low (score = 1), intermediate (score = 2), high (score = 3 to 4), and very high (score = 5 to 6). Transfusion dependency was defined as having at least one

red blood cell (RBC) transfusion every eight weeks over a period of four months.

Statistical analysis

The cumulative probability of survival and risk of progression to leukemia were estimated by using the Kaplan–Meier method. Patients undergoing transplantation treatment were censored at the time of the procedure in order to exclude any potential source of bias due to differential treatment. Variable data were analyzed through Kaplan–Meier methods to estimate the cumulative probabilities of overall survival. The difference in the cumulative probabilities within subcategories of patients was compared by using two-sided log rank test. Survival analyze was performed using Cox proportional model with time-dependent covariates to assess the effect of the variables of interest on overall survival.

Numeric data were evaluated for normal distribution and for equal variance by using the Kolmogorov–Smirnov test and Levene's median test, respectively. Nonparametric data are presented as medians. Categorical data are presented as a percentage of the total or numerically, as appropriate. Statistical comparisons of nonparametric data were compared through the Wilcoxon test. Comparisons of categorical data were made with chi-square or Fischer's exact tests. All tests were two-sided. Statistical significance was indicated by p values of <0.05. Data were analyzed by using SPSS 17.0 software for Windows.

Results

From September 1999 to May 2013, we centrally analyzed for GM-CSF autoantibody in the sera of 619 Japanese cases that had been diagnosed as PAP. Of those cases, 561 were positive for the antibody and 58 were negative. In the cases negative for GM-CSF antibody, 51 demonstrated obvious underlying diseases such as hematological disorders, autoimmune diseases, and infectious diseases. As shown in Figure 1, hematological disorders were the most common underlying disease, 31 cases of which involved MDS. These cases were investigated retrospectively in this study.

Demographic data are shown in Table 1. Diagnosis of MDS was performed in accordance with WHO criteria; 19, 1, 5, 3, and 3 cases were RA, RARS, RCMD, RAEB-1, and RAEB-2, respectively. Karyotyping revealed 2 cases of "high-riskes of g e, 24 cases of "intermediate-riskmediatef, and 5 cases of "low-risks disease. As previously reported [10], there was over-representation of trisomy 8, as it was present in 16 cases (51.6%). RBC transfusion dependency was observed in 11 cases.

PAP was diagnosed on the basis of the BALF and HRCT results in 23 cases and by surgical biopsy and HRCT in eight cases. In 23 cases, diagnosis of MDS was done before diagnosis of PAP, whereas eight cases were diagnosed simultaneously.

According to the WPSS, the cases were classified into 2, 11, 7, 9, and 2 cases of very low-, low-, intermediate-, high-, and very high-risk groups, respectively. For statistical analysis, very low-/low-risk groups and intermediate-/high-/very high-risk groups were categorized as "mild MDS" and "severe MDS" DSere iz, respectively (Table 1). There was no difference in sex and age at the diagnosis of MDS and in hemoglobin concentration, absolute neutrophil count, and platelet count between mild and severe MDS cases. Then, the median age at diagnosis of

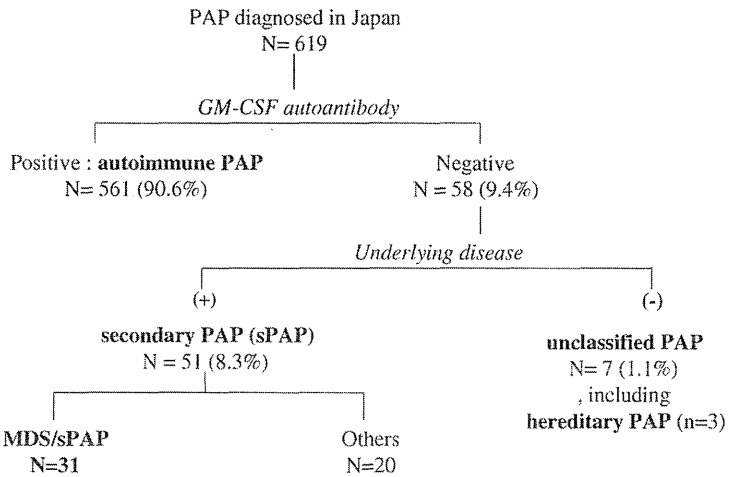

Figure 1 Disposition of patients with pulmonary alveolar proteinosis (PAP) who were enrolled into this study. Participants were stratified according to the presence or absence of granulocyte/macrophage-colony stimulating factor (GM-CSF) autoantibody, and then according to the presence or absence of an underlying disease known to cause PAP.

Table 1 Demographic data at diagnosis of MDS in each group classified according to the WPSS

Median (min.-max.)	Total	<WPSS risk groups>		p value
		<Very low + low >	<Inter − +high + very high>	
		Mild MDS	Severe MDS	
	(n = 31)	(n = 13)	(n = 18)	
Sex (M/F)	19/12	7/6	12/6	0.71
Age at Dx of MDS	50 (27–75)	45 (30–67)	50 (27–75)	0.54
HbG (g/dl)	9.4 (4.8–16.4)	11.4 (5.5–16.4)	9.0 (4.8–13.9)	0.06
ANC ($\times 10^9$/L)	1.84 (0.01–7.54)	1.46 (0.45–6.97)	2.74 (0.01–7.54)	0.68
PLT ($\times 10^9$/L)	65 (6–219)	45 (14–219)	69 (6–196)	0.31
WHO subgroup: n (%)				
RA/RARS	20 (65)	13 (100)	7 (39)	<0.001
RCMD	5 (16)	0 (0)	5 (28)	0.058
RAEB-1,2	6 (19)	0 (0)	6 (33)	0.02
Karyotype*: n (%)				
Good type	2 (7)	2 (15)	0	0.16
Intermediate type	24 (77)	11 (85)	13 (72)	0.66
Poor type	5 (16)	0 (0)	5 (28)	0.058
RBC transfusion dependency**: n (%)	11 (35)	0 (0)	11 (61)	<0.001

(*) Cytogenetics was as follows. Good type: normal, −Y, del(5q), del(20q); poor type: complex (≥ three abnormalities), chromosome 7 anomalies; and intermediate type: other abnormalities.
(**) RBC transfusion dependency was defined as having at least one RBC transfusion every eight weeks over a period of four months. ANC, absolute neutrophil count; Dx, diagnosis; HbG, hemoglobin; MDS, myelodysplastic syndrome; PLT, platelets; RA, refractory anemia; RAEB, refractory anemia with blasts; RARS, refractory anemia with ringed sideroblasts; RBC, red blood cell; RCMD, refractory anemia with multilineage dysplasia; WHO, World Health Organization; WPSS, WHO classification-based prognostic scoring system.

Table 2 Clinical status at death (n = 17)

	No.	WPSS at diagnosis	WHO criteria at diagnosis of MDS	AML progression	Progression of PAP	Pneumonia
				6 (35.3%)	11 (64.7%)	11 (64.7%)
Mild MDS	1	Very low + low	RA			●
	2		RA		●	
	3		RA	●		●
	4		RA		●	●
	5		RA	●		
	6		RA		●	
	7		RA		●	
Severe MDS	8	Intermediate	RA			●
	9		RA		●	●
	10		RA		●	●
	11		RA	●	●	●
	12		RA	●		●
	13		RCMD		●	
	14	High + very high	RA		●	●
	15		RCMD	●	●	
	16		RAEB-1		●	●
	17		RAEB-2	●		●

AML, acute myeloid leukemia; MDS, myelodysplastic syndrome; PAP, pulmonary alveolar proteinosis; RA, refractory anemia; RAEB, refractory anemia with blasts; RCMD, refractory anemia with multilineage dysplasia; WHO, World Health Organization; WPSS, WHO classification-based prognostic scoring system.

MDS/sPAP was 51 years, and 84% of cases were symptomatic, with the most common symptoms being fever (45%), dyspnea on effort (42%), and cough (42%). The value of serum Krebs von den Lungen-6 (KL-6) and surfactant protein-D (SP-D) were elevated, and the diffusing capacities of the lung for carbon monoxide (% DLco) were very low in the absence of ventilation disorder in pulmonary function tests. There was no difference in the frequency of respiratory symptoms between patients with mild MDS and those with severe MDS. Serum biomarkers and pulmonary function tests showed no significant difference between the two groups.

Follow-up periods after diagnosis of MDS ranged from five to 254 months (median, 40 months) in all patients (Additional file 1: Figure S1 and Additional file 2: Figure S2). During the follow-up period, 7 patients with mild MDS and 10 patients with severe MDS died, and 2 patients with mild MDS and 4 patients with severe MDS progressed to AML (Table 2). Two and five patients in the mild MDS and severe MDS groups, respectively, underwent transplantation therapies. They were censored at the time of the procedure. The duration from diagnosis of MDS to diagnosis of sPAP was variable, ranging from 0 to 168 months in the mild MDS group and from 0 to 228 months in the severe MDS group (Figure 2A). The median duration of MDS prior to diagnosis of sPAP in the mild MDS group was significantly longer than that in the severe MDS group

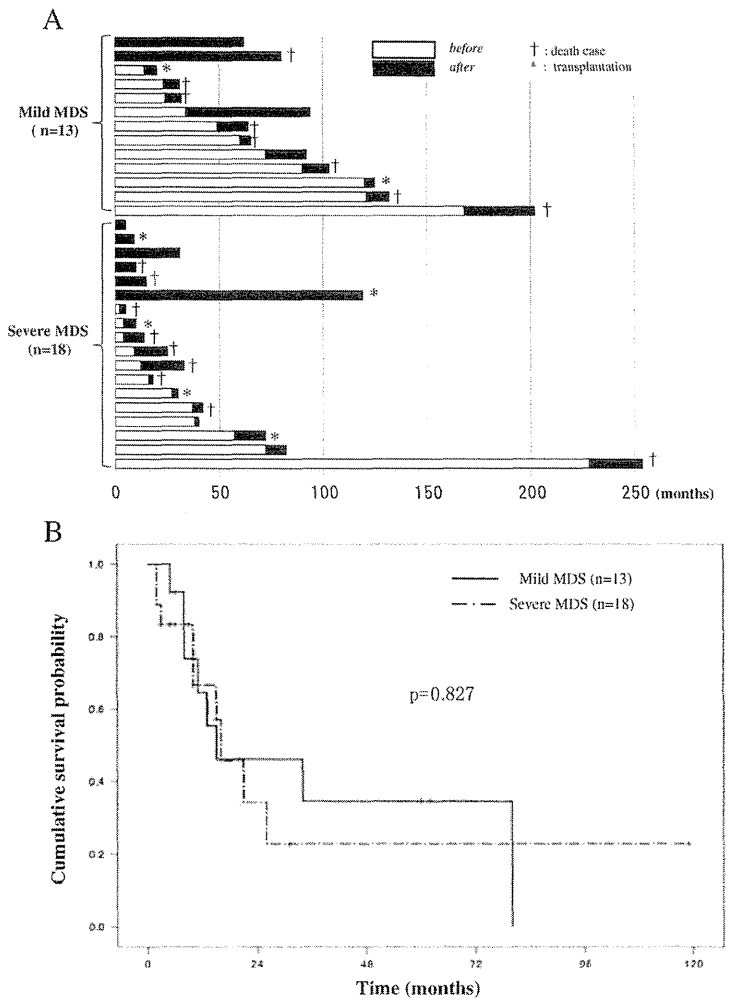

Figure 2 Disease duration of secondary PAP in patients with MDS. A: Duration of disease before or after the diagnosis of secondary pulmonary alveolar proteinosis (sPAP). The horizontal axis indicates the month after the diagnosis of myelodysplastic syndrome. The open column and closed column indicate the duration of disease respectively before and after the diagnosis of sPAP. The case that resulted in death is marked by † and the case that underwent transplantation therapy is marked by *. **B**: Cumulative survival probability after diagnosis of secondary PAP (sPAP) in patient groups with mild myelodysplastic syndrome (MDS) (n = 13) and severe MDS (n = 18). The horizontal axis indicates the month after the diagnosis of sPAP, and the vertical axis indicates the cumulative survival probability.

(p = 0.034). Three patients in the mild MDS group and one in the severe MDS group survived for more than five years after diagnosis of sPAP. Of those, spontaneous remission of sPAP occurred in three cases.

A previous report [7] demonstrated that prediction of survival was dependent on the severity of MDS (as defined by WPSS) at any time of the disease. In contrast, patients with mild MDS in our study had cumulative survival probability similar to that of patients with severe MDS (Figure 2B, p = 0.827). This similarity may be due to poor prognosis of mild MDS after diagnosis of PAP. The cumulative survival probability curves of mild and severe MDS groups with median survivals of 13 and 15 months, respectively, are comparable. Concerning causes for the death of seven patients in the mild MDS group were progression to AML in two cases, PAP exacerbation in four cases, and fatal infectious disease in three cases (Table 2). Concerning causes for the death of 10 patients in the severe MDS group were progression to AML in 4 cases, PAP exacerbation in 7 cases, and fatal infectious disease in 8 cases. Fatal infectious diseases consistently arose from severe pneumonia with (n = 4) or without systemic sepsis, suggesting that progression of PAP was the major cause of death in both mild and severe MDS patients. These results suggest that occurrence of sPAP principally reduced the survival of patients with mild MDS. Pathogens isolated in the fatal cases were identified as *Aspergillus* species (four cases), *Pseudomonas aeruginosa* (four cases), and non-tuberculosis *Mycobacterium* species (four cases).

By performing univariate analysis using Cox proportional model we then searched for potential prognostic factors. Age, sex, respiratory symptoms, history of respiratory failure, diagnostic procedure for sPAP, and MDS group (mild or severe), were not associated with survival at the time of diagnosis of sPAP (Table 3). Treatment with

Table 3 Univariate analysis of overall survival after diagnosis of sPAP in MDS

Variable at diagnosis of sPAP	(n)	75% of OS (months)	50% of OS (months)	HR (95% CI)	P value
Age: 51 yrs or younger	16	8	16		
Older than 52 yrs	15	10	15	1.29 (0.48-3.41)	0.607
Gender: Male	19	10	16		
Female	12	11	21	1.12 (0.43-2.94)	0.804
MDS group: mild	13	10	15		
severe	18	11	16	1.11 (0.42-2.95)	0.830
Symptoms: (−)	5	26	26		
(+)	26	6	15	1.50 (0.33-6.65)	0.592
Dx procedure: Bronchoscopy	23	11	13		
Surgical biopsy	8	15	26	0.69 (0.23-2.04)	0.507
Respiratory failure: (−)	21	11	26		
(+)	10	5	10	2.18 (0.77-6.22)	0.142
Use of corticosteroid: (−)	16	16	80		
(+)	15	10	13	3.20 (1.09-9.38)	0.034
Serum KL-6 (U/ml): < 1960	16	13	26		
1960 ≦	15	5	15	1.52 (0.58-4.00)	0.389
Serum SP-D (ng/ml): < 147	15	10	26		
147 ≦	15	8	15	1.80 (0.62-5.22)	0.278
Serum SP-A (ng/ml): < 79	16	11	26		
79 ≦	14	5	15	2.79 (0.965-8.06)	0.058
%VC: 87 ≦	11	15	34		
< 87	11	8	15	3.27 (0.79-13.52)	0.101
FEV1%: 86 ≦	12	8	16		
< 86	10	13	34	0.52 (0.14-1.87)	0.322
%DLco: 44 ≦	9	21	34		
< 44	8	5	13	9.98 (1.03-96.11)	0.046

CI indicates confidence interval; OS, overall survival; DLco, diffusing capacity of the lung for carbon monoxide; Dx, diagnosis; FEV, forced expiratory volume; HR, hazard ratio; KL-6, krebs von den lungen-6; MDS, myelodysplastic syndrome; SP-A, surfactant protein -A; sPAP, secondary pulmonary alveolar proteinosis; SP-D, surfactant protein -D; VC, vital capacity.

corticosteroids was associated with poor survival (p = 0.024) (Figure 3A). However, the number of patients treated with steroid therapy did not differ between mild and severe MDS groups. A %DLco of <44% (Figure 3B) predicted poor prognosis (p = 0.019), whereas %vital capacity (%VC), forced expiratory volume (FEV) 1.0%, serum KL-6, SP-D, and surfactant protein-A (SP-A) did not.

Discussion

For the first time, we evaluated the prognosis of MDS/sPAP in a substantial cohort of patients, comparing mild and severe MDS as classified according to WPSS criteria. Our data demonstrate that the duration from diagnosis of MDS to diagnosis of sPAP was longer in mild MDS than that in severe MDS, but the survival probability was similar after the diagnosis of sPAP regardless of MDS severity. As a whole, occurrence of PAP appeared to worsen the prognosis of patients with mild MDS. This result is supported by the fact that the major cause of death was not MDS-associated but rather sPAP-associated respiratory failure or infections. Prior to our report, 21 cases with MDS/sPAP have been reported

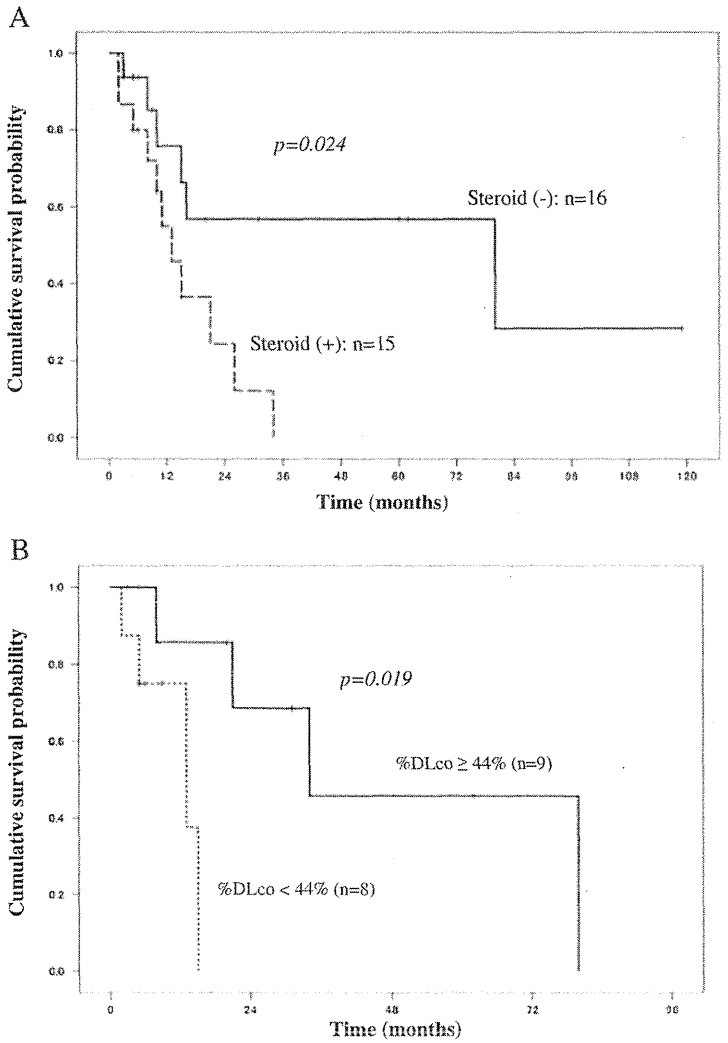

Figure 3 Risk factors for the prognosis of secondary PAP in patients with MDS. A: Cumulative survival probability after diagnosis of secondary PAP (sPAP) in myelodysplastic syndrome (MDS) cases with steroid therapy (n = 15) and in MDS cases without steroid therapy (n = 16). The horizontal axis indicates the month after the diagnosis of sPAP, and the vertical axis indicates the cumulative survival probability. The number of cases that received steroid therapy in the mild and severe MDS groups were six (46%) and nine (59%), respectively. **B**: Cumulative survival probability after diagnosis of secondary PAP (sPAP) in myelodysplastic syndrome (MDS) cases with diffusing capacity of the lung for carbon monoxide (%DLco) of <44% (n = 8) and in MDS cases with%DLco of >44% (n = 9). The horizontal axis indicates month after the diagnosis of sPAP, and the vertical axis indicates the cumulative survival probability.

[8-18]. Most reports [9-18,21-24] describe a single case, whereas only two publications report multiple cases [8,25]. The clinical course described in these reports suggest a poor prognosis for MDS/sPAP patients, but no prior report clearly quantifies the outlook for these patients and compares this to a predicted outcome by using validated prognostic scores such as WPSS. MDS/sPAP is so rare a disease that neither pulmonologists nor hematologists encounter such patients very often. In fact, in more than 10 years, 2 to 5 cases were diagnosed as MDS/sPAP annually in our analyses for serum GM-CSF autoantibody in over 600 diagnosed PAP cases from all over Japan; thus, we have finally reached cumulative 31 cases with MDS/sPAP.

According to the WHO criteria, 20 of the 31 cases were RA/RARS, 5 cases were RCMD, and 6 cases were RAEB1-2. The proportion of the number for each subtype in the total number of cases was comparable to literature data in terms of frequency and subtype distribution, suggesting that the risk of PAP complicating MDS is similar regardless of the subtype of MDS. It is speculated that AMs in patients with MDS derive from abnormal bone marrow precursor cells and are defective in both surfactant homeostasis and host defense, hence the progression of PAP and PAP-associated infections even in cases with mild MDS. Previous studies reported that in the absence of complicating sPAP, the five-year survival probability for patients with RA and RARS was 74% [26], whereas our cases with RA plus RARS had substantially inferior prognosis (0.69) (Additional file 2: Figure S2).

It is noteworthy that treatment with corticosteroids was associated with a markedly inferior prognosis. In Japan, steroid therapy often has been used for PAP but no evidence of its efficacy has been found. To our surprise, 15 of 31 cases had undergone steroid therapy during the course of sPAP. Our data reveal that steroid-treated patients had worse prognosis than did patients without steroid therapy. Given that the predominant cause of death was infective complications potentially exacerbated by steroid-related immunosuppression, these data clearly caution against the use of steroid therapy in such patients.

Treatment of MDS/sPAP should be directed toward the underlying malignancy, i.e., MDS. It should also aim at restoring hematopoietic function, either through allogeneic bone marrow transplant, which has curative potential for both MDS and sPAP, or through hypomethylating agent therapy for MDS, which can restore numerical hematologic parameters. However, functional cellular defects will likely remain, as such therapy does not necessarily eradicate the underlying clone, but rather enhances cellular differentiation [27,28]. Nevertheless, seven cases with MDS/sPAP to date in our cohort had undergone transplantation therapy. Of those, three patients died of pneumonia within three months of the transplantation therapy. Therefore, we do not have any convincing evidence to recommend transplantation therapy in the early stages of the disease. Although whole-lung lavage and segmental bronchial lavage were performed in 10 patients, only 3 cases showed the efficacy of lung-lavage therapy.

Infection often coexists with MDS/sPAP, although the causal relationship between PAP and infection is not clear. Superimposed infection accounts for a significant degree of morbidity and mortality in patients with sPAP. In the present study, 11 among 17 cases with fatal outcomes developed fatal infectious diseases. Considering that this complication was observed in the mild MDS and severe MDS groups, pneumonia accompanied with sPAP might be the trigger of fatal infection. Nevertheless, the present number of cases (31) is too small for accurate prognosis evaluation of MDS/sPAP; future international collaboration may be necessary to overcome this difficulty.

Conclusions

Complication of sPAP is an important risk factor in the prognosis of MDS. We believe that the present data will contribute to the management and treatment of the disease.

Additional files

Additional file 1: Figure S1. Survival curves after diagnosis of MDS in each mild and severe MDS.

Additional file 2: Figure S2. Survival curves in each MDS groups classified by WHO-criteria.

Abbreviations

AM: Alveolar macrophage; AML: Acute myeloid leukemia; ANC: Absolute neutrophil count; BALF: Bronchoalveolar lavage fluid; CEA: Carcinoembryonic antigen; CT: Computed tomography; DLco: Diffusing capacity of the lung for carbon monoxide; Dx: Diagnosis; FEV: Forced expiratory volume; GM-CSF: Granulocyte macrophage colony-stimulating factor; HbG: Hemoglobin; HRCT: High-resolution computed tomography; KL-6: Krebs von den Lungen-6; MDS: Myelodysplastic syndrome; PAP: Pulmonary alveolar proteinosis; PLT: Platelets; RA: Refractory anemia; RARS: Refractory anemia with ringed sideroblasts; RAEB: Refractory anemia with blasts; RBC: Red blood cell; RCMD: Refractory anemia with multilineage dysplasia; SD: Standard deviation; SP-A: Surfactant protein-A; sPAP: Secondary pulmonary alveolar proteinosis; SP-D: Surfactant protein-D; VC: Vital capacity; WHO: World Health Organization; WPSS: WHO classification-based prognostic scoring system.

Competing interests

Financial/non-financial competing interests

The authors report no potential conflicts of interest with any companies or organizations whose products or services are mentioned in this article.

Authors' contributions

The authors take responsibility and vouch for the completeness and accuracy of the data and analyses. HI and KN are the guarantors of the entire manuscript. HI and JS contributed to the study concept and design, coordination of data acquisition, and writing of the article. RT, YI, NU, AN, YK,

and TS contributed to the data analysis. KT, TT, YI, MH, TI, and HG contributed to the interpretation of the data and writing of the article. KN participated in writing and critically revising the manuscript. All authors read and approved the final manuscript.

Acknowledgments

The authors thank Dr. Sato J., Matsui T., Yoshioka Y., Shijubo N., Hara H., Amitani K., Takahashi S., Fukuno K., Handa T., Nakatsue T., Saito Y., Asai Y., Ohkochi Y., Saito Y., Yasui T., Baba M., Yanai H., Tanino T., Setoguchi Y., Yamamoto S., Ohkochi S., Morita M., Hashimoto K., Matsumoto K., and Komeno T. for providing patient samples and information. We also thank Takizawa J., Sone H., Akira M., and Kitamura N. for valuable discussions and suggestions, and Mori M. for technical help. Our work was partially supported by a grant from Category C23591160, B24390208, and B12023059 from the Japan Society for the Promotion of Science. This research was also supported by a grant from the Ministry of Health, Labour, and Welfare (H24, Nanchi-ippan-035, and H24 Rinken Sui-003). The sponsor had no role in the study design, data collection and analysis, and manuscript preparation.

Author details

[1]Department of Respiratory Medicine, Kyorin University School of Medicine, 6-20-2 shinkawa, Mitaka-shi, Tokyo 1818611, Japan. [2]Department of Haematology, Peter MacCallum Cancer Centre, St Andrews Place, East Melbourne, Victoria 8006, Australia. [3]Bioscience Medical Research Center, Niigata University Medical & Dental Hospital, 1-754 Asahimachi-dori, Chuo-ku, Niigata 9518520, Japan. [4]Diffuse Lung Diseases and Respiratory Failure, Clinical Research Center, NHO Kinki-Chuo Chest Medical Center, 1180 Nagasone-cho, Kita-ku, Sakai, Osaka 5918555, Japan. [5]Department of Hematology, Toranomon Hospital, 2-2-2 Toranomon, Minato-ku, Tokyo 1058470, Japan. [6]Department of Respiratory Medicine, NHO Nagoya Medical Center, 4-1-1 Sannomal, Naka-ku, Nagoya, 4600001Japan. [7]Department of Pulmonary Medicine, Kobe City General Hospital, 4-6 Minatojimanakamachi, Chuo-ku, Kobe-city, Hyogo 6500046, Japan. [8]Division of Respiratory Medicine, Niigata University Graduate School of Medical and Dental Sciences, 1-754 Asahimachi-dori, Chuo-ku, Niigata 9518520, Japan. [9]Division of Respiratory Medicine, National Center for Global Health and Medicine, 1-21-1 Toyama, Shinjuku-ku, Tokyo 1628655, Japan. [10]Department of Respiratory Medicine, Tokyo Medical University Hachioji Medical Center, 1163 Tatemachi, Hachioji-shi, Tokyo 1930998, Japan.

Received: 8 December 2013 Accepted: 24 February 2014
Published: 5 March 2014

References

1. Rosen SH, Castleman B, Liebow AA: **Pulmonary alveolar proteinosis.** *N Engl J Med* 1958, **258**:123–1143.
2. Seymour JF, Presneill JJ: **Pulomary alveolar proteinosis: progress in the first 44 years.** *Am J Respir Crit Care Med* 2002, **166**:215–235.
3. Kitamura T, Tanaka N, Watanabe J, Uchida K, Kanegasaki S, Yamada Y, Nakata K: **Idiopathic pulmonary alveolar proteinosis as an autoimmune disease with neutralizing antibody against granulocyte-macrophage colony stimulating factor.** *J Exp Med* 1999, **190**:875–880.
4. Ishii H, Tazawa R, Kaneko C, Saraya T, Inoue Y, Hamano E, Kogure Y, Tomii K, Terada M, Takada T, Hojo M, Nishida A, Ichiwata T, Trapnell BC, Goto H, Nakata K: **Clinical features of secondary pulmonary alveolar proteinosis: pre-mortem cases in Japan.** *Eur Respir J* 2011, **37**:465–468.
5. Cazzola M, Malcovati L: **Myelodysplastic syndrome: coping with ineffective hematopoiesis.** *N Engl J Med* 2005, **352**:536–538.
6. Vardiman JW, Harris NL, Brunning RD: **The World Health Organization (WHO) classification of the myeloid neoplasms.** *Blood* 2002, **100**:2292–2302.
7. Malcovati L, Germing U, Kuendgen A, Della Porta MG, Pascutto C, Invernizzi R, Giagounidis A, Hildebrandt B, Bernasconi P, Knipp S, Strupp C, Lazzarino M, Aul C, Cazzola M: **Time-dependent prognostic scoring system for predicting survival and leukemic evolution in myelodysplastic syndrome.** *J Clin Oncol* 2007, **25**:3503–3510.
8. Nishida A, Miyamoto A, Yamamoto H, Uchida N, Izutsu K, Wake A, Ohta Y, Fujii T, Araoka H, Taniguchi S, Kishi K: **Possible association of trisomy 8 with secondary pulmonary alveolar proteinosis in myelodysplastic syndrome.** *Am J Respir Crit Care Med* 2011, **184**:279–280.
9. Asai Y, Ouchi H, Ohosima T, Nakano R, Yamano Y, Inoshima I, Yamauchi T, Fukuyama S, Inoue H, Nakanishi Y: **A case of secondary pulmonary alveolar proteinosis associated with myelodysplastic syndrome, complicated with disseminated *M. abscessus* infection.** *Nihon Kokyuki Gakkai Zasshi* 2009, **47**:1120–1125.
10. Tabata S, Shimoji S, Murase K, Takiuchi Y, Inoue D, Kimura T, Nagai Y, Mori M, Togami K, Kurata M, Ito K, Hashimoto H, Matushita A, Nagai K, Takahashi T: **Successful allogeneic bone marrow transplantation for myelodysplastic syndrome complicated by severe pulmonary alveolar proteinosis.** *Int J Haemol* 2009, **90**:407–412.
11. Fukuno K, Tomonari A, Tsukada N, Takahashi S, Ooi J, Konuma T, Uchiyama M, Fujii T, Endo T, Iwamoto A, Oyaizu N, Nakata K, Moriwaki H, Tojo A, Asano S: **Successful cord blood transplantation for myelodysplastic syndrome resulting in resolution of pulmonary alveolar proteinosis.** *Bone Marrow Transplant* 2006, **38**:581–582.
12. Ohnishi T, Yamada S, Shijubo N, Takagi-Takahashi Y, Itoh T, Takahashi H, Satoh M, Koba H, Nakata K, Abe S: **Secondary pulmonary alveolar proteinosis associated with myelodysplastic syndrome.** *Intern Med* 2003, **42**:187–190.
13. Yokomura K, Chida K, Suda T, Miwa S, Nakano H, Kuwata H, Suzuki K, Matsuda H, Asada K, Nakamura Y, Inui N, Shirai M, Suzuki K, Nakamura H: **Secondary pulmonary alveolar proteinosis associated with myelodysplastic syndrome.** *Nihon Kokyuki Gakkai Zasshi* 2002, **40**:599–604.
14. Yoshioka Y, Ohwada A, Harada N, Satoh N, Sakuraba S, Dambara T, Fukuchi Y: **Increased circulating CD16+ CD14dim monocytes in a patient with pulmonary alveolar proteinosis.** *Respirology* 2002, **7**:273–279.
15. Ito T, Yoshii C, Imanaga T, Hayashi T, Kawanami K, Kido M: **A case of pulmonary alveolar proteinosis complicated with pneumoconiosis and myelodysplastic syndrome.** *Nihon Kokyuki Gakkai Zasshi* 2001, **39**:710–715.
16. Kajiume T, Yoshimi S, Nagita A, Kobayashi K, Kataoka N, Nakajima M, Matsushima T: **A case of myelodysplastic syndrome complicated by pulmonary alveolar proteinosis with a high serum KL-6 level.** *Pediatr Hematol Oncol* 1999, **16**:367–371.
17. Terashima T, Nakamura H, Meguro S, Fujimori H, Yamaguchi K, Kanazawa M, Kato R, Kobayashi K: **Pulmonary alveolar proteinosis associated with myelodysplastic syndrome.** *Nihon Kokyuki Gakkai Zasshi* 1995, **33**:645–651.
18. Nakata K, Tamura T, Aikawa K, Yoshida H, Mikuni O, Inoue M, Nasuhara K: **A case of pulmonary alveolar proteinosis complicated with myelodysplastic syndrome.** *Nihon Naki Gakkai Zasshi* 1991, **80**:106–107.
19. Standing Committee on Human Cytogenetics Nomenclature: **ISCN: an international system for human cytogenetic nomenclature-report of the standing committee on human cytogenetic nomenclature.** *Birth Defects Orig Ser* 1985, **21**:1–117.
20. Greenberg P, Cox C, Lebeau MM, Fenaux P, Morel P, Sanz M, Vallespi T, Hamblin T, Oscier D, Ohyashiki K, Toyama K, Aul C, Mufti G, Bennett J: **International scoring system for evaluating prognosis in myelodysplastic syndromes.** *Blood* 1997, **8**:2079–2088.
21. Xue Y, Han Y, Li T, Chen S, Zhang J, Pan J, Wu Y, Wang Y, Shen J: **Pulmonary alveolar proteinosis as a terminal complication in a case of myelodysplastic syndrome with idic(20q-).** *Acta Haematol* 2010, **123**:55–58.
22. Chung JH, Pipavath SJ, Myerson DH, Godwin D: **Secondary pulmonary alveolar proteinosis: a confusing and potentially serious complication of hematologic malignancy.** *J Thorac Imaging* 2009, **24**:115–118.
23. Xie LX, Zhao TM, Wang QY, Chen LA, Li AM, Wang DJ, Qi F, Liu YN: **Secondary pulmonary alveolar proteinosis associated with myelodysplastic syndrome.** *Chin Med J* 2007, **120**:1114–1116.
24. Pollack SM, Gutierrez G, Ascensao J: **Pulmonary alveolar proteinosis with myeloprolifereative syndrome with myelodysplasia: bronchoalveolar lavage reduces white blood cell count.** *Am J Hematol* 2006, **81**:634–638.
25. Shoji N, Ito Y, Kimura Y, Nishimaki J, Kuriyama Y, Tauchi T, Yamaguchi M, Payzulla D, Ebihara Y, Ohyashiki K: **Pulmonary alveolar proteinosis as a terminal complication in myelodysplastic syndrome: a report of four cases detected on autopsy.** *Leuk Res* 2002, **26**:591–595.
26. Malcovati L, Porta GD, Pascutto C, Invernizzi R, Boni M, Travaglino E, Passamonti F, Arcaini L, Maffioli M, Bermasconi P, Lazzarino M, Cazzola M: **Prognostic factors and life expectancy in myelodysplastic syndromes classified according to WHO criteria: a basis for clinical decision making.** *J Clin Oncol* 2005, **23**:7594–7603.
27. Fenaux P, Mufti GJ, Hellstrom-Lindberg E, Santini V, Finelli C, Giagounidis A, Schoch R, Gattermann N, Sanz G, List A, Gore SD, Symour JF, Bennett JM,

Byrd J, Backstrom J, Zimmerman L, Mckenzie D, Beach C, Silverman LR: Efficacy of azacitidine compared with that of conventional care regimens in the treatment of higher-risk myelodysplastic syndromes: a randomized, open-label, phase III study. *Lancet Oncol* 2009, 10(3):223–232.

28. Gangatharan SA, Carney DA, Campbell LJ, Prince HM, Kenealy MK, Seymour JF: Cytogenetic response is not a prerequisite for clinical response in patients with myelodysplastic syndromes treated with azacitidine. *Eur J Haematol* 2011, 87(2):186–188.

doi:10.1186/1471-2466-14-37
Cite this article as: Ishii *et al.*: Secondary pulmonary alveolar proteinosis complicating myelodysplastic syndrome results in worsening of prognosis: a retrospective cohort study in Japan. *BMC Pulmonary Medicine* 2014 14:37.

Am J Physiol Lung Cell Mol Physiol 308: L105–L117, 2015.
First published November 14, 2014; doi:10.1152/ajplung.00239.2014.

CALL FOR PAPERS | *Bioengineering the Lung: Molecules, Materials, Matrix, Morphology, and Mechanics*

A mathematical model to predict protein wash out kinetics during whole-lung lavage in autoimmune pulmonary alveolar proteinosis

Keiichi Akasaka,[1] Takahiro Tanaka,[1] Takashi Maruyama,[2] Nobutaka Kitamura,[1] Atsushi Hashimoto,[1] Yuko Ito,[1] Hiroyoshi Watanabe,[3] Tomoshige Wakayama,[3] Takero Arai,[4] Masachika Hayashi,[5] Hiroshi Moriyama,[5] Kanji Uchida,[6] Shinya Ohkouchi,[7] Ryushi Tazawa,[1] Toshinori Takada,[8] Etsuro Yamaguchi,[9] Toshio Ichiwata,[10] Masaki Hirose,[11] Toru Arai,[11] Yoshikazu Inoue,[11] Hirosuke Kobayashi,[12] and Koh Nakata[1]

[1]*Bioscience Medical Research Center, Niigata University Medical and Dental Hospital, Niigata, Japan;* [2]*Disaster Prevention Research Institute, Kyoto University, Kyoto, Japan;* [3]*Department of Respiratory Medicine, Dokkyo Medical University Koshigaya Hospital, Saitama, Japan;* [4]*Department of Anesthesiology, Dokkyo Medical University Koshigaya Hospital, Saitama, Japan;* [5]*Division of Respiratory Medicine, Niigata University Medical and Dental Hospital, Niigata, Japan;* [6]*Department of Anesthesiology, Graduate School of Medicine, The University of Tokyo, Tokyo, Japan;* [7]*Department of Respiratory Medicine, Tohoku University Graduate school of Medicine, Miyagi, Japan;* [8]*Uonuma Institute of Community Medicine, Niigata University Medical and Dental Hospital, Niigata, Japan;* [9]*Department of Respiratory and Allergy Medicine, Aichi Medical University, Aichi, Japan;* [10]*Department of Pulmonary Medicine, Tokyo Medical University Hachioji Medical Center, Tokyo, Japan;* [11]*Clinical Research Center, NHO Kinki-Chuo Chest Medical Center, Osaka, Japan; and* [12]*Graduate School of Medical Sciences, Kitasato University, Kanagawa, Japan*

Submitted 4 September 2014; accepted in final form 10 November 2014

Akasaka K, Tanaka T, Maruyama T, Nobutaka Kitamura, Hashimoto A, Ito Y, Watanabe H, Wakayama T, Arai T, Hayashi M, Moriyama H, Uchida K, Ohkouchi S, Tazawa R, Takada T, Yamaguchi E, Ichiwata T, Hirose M, Arai T, Inoue Y, Kobayashi H, Nakata K. A mathematical model to predict protein wash out kinetics during whole-lung lavage in autoimmune pulmonary alveolar proteinosis. *Am J Physiol Lung Cell Mol Physiol* 308: L105–L117, 2015. First published November 14, 2014; doi:10.1152/ajplung.00239.2014.—Whole-lung lavage (WLL) remains the standard therapy for pulmonary alveolar proteinosis (PAP), a process in which accumulated surfactants are washed out of the lung with 0.5–2.0 l of saline aliquots for 10–30 wash cycles. The method has been established empirically. In contrast, the kinetics of protein transfer into the lavage fluid has not been fully evaluated either theoretically or practically. Seventeen lungs from patients with autoimmune PAP underwent WLL. We made accurate timetables for each stage of WLL, namely, instilling, retaining, draining, and preparing. Subsequently, we measured the volumes of both instilled saline and drained lavage fluid, as well as the concentrations of proteins in the drained lavage fluid. We also proposed a mathematical model of protein transfer into the lavage fluid in which time is a single variable as the protein moves in response to the simple diffusion. The measured concentrations of IgG, transferrin, albumin, and β_2-microglobulin closely matched the corresponding theoretical values calculated through differential equations. Coefficients for transfer of β_2-microglobulin from the blood to the lavage fluid were two orders of magnitude higher than those of IgG, transferrin, and albumin. Simulations using the mathematical model showed that the cumulative amount of eliminated protein was not affected by the duration of each cycle but dependent mostly on the total time of lavage and partially on the volume instilled. Although physicians have paid little attention to the transfer of substances from the lung to lavage fluid, WLL seems to be a procedure that follows a diffusion-based mathematical model.

pulmonary alveolar proteinosis; granulocyte/macrophage colony-stimulating factor autoantibody; whole-lung lavage; protein transfer rate

PULMONARY ALVEOLAR PROTEINOSIS (PAP) is a rare lung disorder in which surfactant-associated phospholipids and proteins abnormally accumulate within alveoli and terminal bronchioles, leading to impaired gas exchange and progressive respiratory failure (6, 33, 40). PAP is classified into three groups based on etiology: autoimmune PAP (aPAP), secondary PAP, and hereditary PAP (6, 17, 40). aPAP is caused by granulocyte/macrophage colony-stimulating factor (GM-CSF) autoantibodies, which prevent surfactant removal by alveolar macrophages (20, 41). aPAP is the most prevalent form of PAP, comprising 90% of all PAP cases (6, 17, 40). Currently, whole-lung lavage (WLL) remains the only standard therapy for aPAP (4, 7, 29). Although WLL improves PAP in about 85–95% of patients, around 15–66% of such patients may require multiple and repeated WLL therapy (1, 4, 37). Removal of the lipoproteinous material by WLL immediately improves both lung volume and ventilation/perfusion ratio, leading to a marked increase in arterial oxygen gas pressure (5, 29, 36). In contrast, the diffusion capacity recovers gradually and incompletely over a 6-mo period (36). In addition, WLL decreases the area of ground-glass opacities but not reticular opacities and inter-

Address for reprint requests and other correspondence: K. Nakata, Bioscience Medical Research Center, Niigata Univ. Medical and Dental Hospital, 1-754 Asahimachi-dori, Niigata 951-8520, Japan (e-mail: radical@med.niigata-u.ac.jp)

lobular septal thickening (24). These observations suggest that the efficacy of WLL is not attributable to simple exclusion of accumulated surfactants but rather attributable to the recovery of normal lung structure and function.

GM-CSF autoantibodies and various other proteins (with the exception of large molecules such as IgM) have been reported to transfer the air-blood barrier (2, 9, 39). Both IgG1/albumin and IgG2/albumin ratios of the serum and bronchoalveolar lavage fluid (BALF) are similar, indicating transfer of these proteins (28). IgG most probably migrates by epithelial transcytosis or by paracellular diffusion through the air-blood barrier (13). In the steady state, the air-blood barrier consists of endothelial cells, basement membrane, epithelial cells, and surfactant film (8, 15). Surfactant film reduces leakage of plasma proteins to a minimum (15). In a previous study, disruption of surface tension-lowering properties of surfactant protein B (SP-B) in conditional knockout mice led to constriction of alveolar capillaries that resulted in protein leaks, lung edema, and alterations in alveolar surface area (15). Although no report describes the disruption of air-blood barrier after lung lavage, it is plausible that WLL removes the surfactant film from the alveolar surface followed by leaking plasma proteins.

In the present study, the kinetics of transfer of proteins from the blood and the surfactant to the lavage fluid was examined by measuring their concentrations in aliquots of lavage fluid drained during WLL. For this purpose, we proposed a mathematical model that can account for the transfer of proteins from the blood and the surfactant to the lavage fluid. The transmission coefficients were optimized, and the temporal variations of protein concentrations were simulated. Finally, the proposed model was evaluated by comparison with the measured data. Moreover, we showed the limitations of the present model.

Glossary

A_b	The effective surface area from the blood
A_s	The effective surface area from the surfactant
K_b	The transmission coefficient from the blood
K_s	The transmission coefficient from the surfactant
m_b	The masses of protein in the blood
$m_{in\text{-}out}$	The masses of protein in instilling saline and draining lavage fluid; actually, no protein exists in instilling saline
m_l	The masses of protein in the lavage fluid
m_{out}	The protein mass of drainage
m_s	The masses of protein in the surfactant
R_{cl}	The absorption rate of fluid into the circulation
S_A	The alveolar surface area
V_A	The alveolar volume
V_b	The volume of blood
V_{in}	The fluid volume of instilled saline
V_l	The volume of lavage
$V_{l\text{-}b}$	The fluid volume absorbed into the circulation
V_{out}	The fluid volume of drainage
V_s	The volume of surfactant

MATERIALS AND METHODS

Participants

Nine patients were enrolled in five hospitals in Japan. These hospitals included Tohoku University Hospital, Tokyo Medical University Hachioji Hospital, Aichi Medical University Hospital, Dokkyo Medical University Koshigaya Hospital, and Niigata University Medical and Dental Hospital. Diagnosis of aPAP was performed on the basis of cytological analysis of BALF, pulmonary histopathological findings, or both with high-resolution computed tomography appearance (40). All cases were confirmed to have elevated serum GM-CSF autoantibody levels (21, 41). The institutional review board of each hospital approved the study, and all subjects provided written informed consent. The study protocol was designed according to The Ethical Guideline of Clinical Research by The Japanese Ministry of Health, Labour, and Welfare in 2008.

Data of arterial blood gas analyses and serum markers were collected within 3 days, and pulmonary function tests were within 2 wk prior to WLL.

Procedure of WLL

Seventeen lungs from nine patients with aPAP underwent WLL. We allowed each participating hospital to conduct WLL in accordance with their own procedures. Generally, after administration of general anesthesia, patients were intubated with a double-lumen endotracheal tube to isolate the lungs, after which mechanical ventilation was initiated. After ventilation of the bilateral lungs with 100% oxygen for 5–15 min, saline was instilled into the lavage lung while ventilation of the other lung with 100% oxygen was continued. The instilled saline was then retained for a few minutes and then discharged by gravity into a container until a decrease in outflow was observed. These procedures were then repeated. In each lavage cycle, we prepared a timetable to record the exact time (to the second) of the start of instilling saline, the start of retaining, and the start and end of lavage fluid draining. We measured the volume of drained lavage fluid and used a 10-ml aliquot for further analyses. All samples were stored at −80°C until use.

Measurement of Substance Concentration

The serum and BALF concentration of IgG, GM-CSF autoantibody, transferrin, albumin, β_2-microglobulin, urea, gastrin, and SP-D were measured; IgG were quantified by an ELISA system using Human IgG ELISA Quantitation Set (Bethyl Laboratories, Montgomery, AL) according to the manufacturer's instructions. GM-CSF autoantibody concentrations were measured by an ELISA system as described previously (17). β_2-Microglobulin, gastrin, urea, and SP-D concentrations were measured by latex agglutination immunoassay (LA; LZ test Eiken β_2-M-II; Eiken, Tokyo Japan), radioimmunoassay (gastrin RIA kit II; Fujirebio, Tokyo, Japan), urease-indophenol method (urea nitrogen test; Wako, Tokyo, Japan), and enzyme immunoassay (SP-D kit Yamasa EIA II; Yamasa, Tokyo, Japan), respectively. Serum transferrin and albumin concentrations were measured by turbidimetric immunoassay (TIA; N-Assay TIA Tf-H Nittobo; Nittobo, Tokyo, Japan) and bromocresol purple dye-binding assay (PureAuto A ALB; Kainos, Toyko, Japan), respectively, and those in the BALF were analyzed by LA (N-Assay LA Micro Tf Nittobo) and TIA (AutoWako Microalbumin). These serum samples were collected just before the beginning of WLL.

A Mathematical Kinetic Model to Estimate the Concentration of Proteins in the Lavage Fluid

We postulated that proteins both in the accumulated surfactant material and in the pulmonary capillaries transfer into the lavage fluid. Under such circumstances, the rate of protein transfer to the lavage fluid is assumed to be as follows:

$$\frac{dm_l}{dt} = \frac{dm_s}{dt} + \frac{dm_b}{dt} + \frac{dm_{in-out}}{dt} \quad (1)$$

where the first term in the right-hand side is the transfer rate from surfactant, the second term is the transfer rate from blood, and the

third term is the rate of instilling and drainage. The transfer rate from surfactant dm_s/dt and the transfer rate from blood dm_b/dt are modeled by analogy to the heat transmission model as

$$\frac{dm_s}{dt} = K_S \cdot A_S \left(\frac{m_s}{V_s} - \frac{m_l}{V_l}\right) \quad (2)$$

$$\frac{dm_b}{dt} = K_b \cdot A_b \left(\frac{m_b}{V_b} - \frac{m_l}{V_l}\right) \quad (3)$$

where K_s and K_b are the transmission coefficient from the surfactant and the blood to the lavage fluid, respectively. A_s and A_b are the effective surface area from the surfactant and the blood to the lavage fluid, respectively. The parameters m_l, m_s, and m_b represent the masses of protein in the lavage fluid, surfactant, and blood, respectively. V_l represents the fluid volume in lavage. V_s and V_b represent the fluid volume in surfactant and blood. We assumed that m_b, V_s, and V_b are constant during the WLL.

We calculated the temporal variation of the mass of protein and the volume of fluid in the stages of instilling, retaining, draining, and preparing in each lavage cycle, as described as follows.

Instilling stage. The volume change of protein and lavage fluid in the lung is expressed as:

$$\frac{dm_{in-out}}{dt} = 0 \quad (4)$$

$$\frac{dV_l}{dt} = \frac{dV_{in}}{dt} - \frac{dV_{l-b}}{dt} \quad (5)$$

where V_{in} is the fluid volume of instilled saline, and V_{l-b} is the fluid volume absorbed into the circulation expressed as

$$\frac{dV_{l-b}}{dt} = A_b \cdot R_{cl} \quad (6)$$

where R_{cl} is the absorption rate of fluid into the circulation. The concentration of protein was calculated as the ratio of the mass of protein to the fluid volume calculated from *Eqs. 1–6* according to the procedures described in the following subsection.

Retaining stage. No saline is instilling in the retaining stage, which means

$$\frac{dV_{in}}{dt} = 0 \quad (7)$$

The variation of the mass of protein and the volume of fluid were calculated from *Eqs. 1–7*.

Draining stage. The lavage fluid is drained in this stage, which means

$$\frac{dm_{in-out}}{dt} = -\frac{dm_{out}}{dt} \quad (8)$$

$$\frac{dV_l}{dt} = -\frac{dV_{out}}{dt} - \frac{dV_{l-b}}{dt} \quad (9)$$

where m_{out} and V_{out} are the protein mass and the fluid volume of drainage. The variation of the mass of protein and the volume of fluid were calculated from *Eqs. 1–3* and *6*, *8*, and *9*.

Preparing stage. Substance transfer in this stage may be considered to be similar to that in the retaining stage.

Data Processing and Statistics

Data including patient identity, protein concentrations in the serum or in the BALF of the right and left lungs, vital capacity, the number of cycles, the volume of instilled saline or drained lavage fluid, and time for each lavage stage were entered into a file (Microsoft Excel 2010). Using theoretical equations that solved protein concentrations in the drained lavage fluid (described in RESULTS), we wrote a program using Visual Basic Application to calculate the theoretical concentrations of proteins on the basis of specific variables.

Estimation of the protein concentration in the drained lavage fluid was carried out by numerically integrating differential equations using the following parameters: the volume of instilled saline, drained lavage fluid, time of each stage, the concentration of proteins in the first lavage cycle, effective alveolar and capillary surface area described below, and a given set of transmission coefficients, K_s and K_b. The resulting concentration curve was optimized with actual measurements manually by changing transmission coefficients. The effective areas of alveolar surface and pulmonary capillaries were calculated according to the equations described in Appendix A (10).

Numerical data were evaluated for normal distribution by using Shapiro-Wilk tests. Nonparametric data were analyzed by using Kruskal-Wallis rank sum test. Multiple comparisons were performed through a Bonferroni-adjusted Wilcoxon rank-sum test. All tests were two-sided, and P values <0.05 were considered statistically significant. Data were analyzed by using R-version 2.15.2 (R Foundation for Statistical Computing, Vienna, Austria).

RESULTS

Demographic and Clinical Findings for Study Subjects

Nine patients with active aPAP were enrolled in this study. Demographic data are shown in Table 1.

The mean age at WLL was 54.3 ± 11.4 yr old, with a male-to-female ratio of 2:1. The duration of the disease from onset was variable, ranging 10–96 mo. Patients showed no evidence of active pulmonary infection. Pulmonary functions and laboratory findings are described in Table 2.

The mean arterial oxygen pressure at room air was 64.0 ± 15.4 mmHg in seven patients and 55.2 and 67.4 mmHg for two patients under nasal oxygen supply. Percentage of vital capacity and percentage of carbon monoxide diffusing capacity were moderately to severely suppressed with 72.1 ± 17.7% and 51.0 ± 21.5%, respectively, whereas forced expiratory volume in 1 s/forced vital capacity was relatively conserved with 85.8 ± 10.9%. The mean serum biomarker levels of Krebs von den Lungen-6, SP-D, and carcinoembryonic antigen were 20,720 ± 13,953 IU/ml, 471 ± 271 ng/ml, and 26.7 ± 22.9 ng/ml, respectively. The mean serum GM-CSF autoantibody levels were 45.8 ± 51.7 μg/ml. These patient characteristics were similar to a past large Japanese cohort with PAP (17).

Timetables and Volume Balance for WLL

As shown in Fig. 1, *A* and *B*, each lavage cycle consisted of four stages: instilling (from the beginning to the end of saline instillation), retaining (from the end of saline instillation until the beginning of drainage), draining (from the beginning until the end of drainage), and preparing (from the end of drainage until the beginning of the next saline instillation). Twelve lungs from seven patients underwent WLL with short-term cycles (210–285 s), whereas five lungs from three patients underwent WLL with long-term cycles (550–634 s) (Table 3). In eight patients, both lungs underwent WLL: however, for one patient, only the right lung underwent lavage. Data for instilled saline volume, discharged lavage fluid volume, and time for each of the stages as defined above are shown in Tables 3 and 4. Lavage was repeated 11 to 29 times (median of 20 cycles) until the lavage fluid appeared clearer (Fig. 1*C*).

Time required for total WLL time ranged from 5,200 to 11,796 s. Instilling, retaining, draining, and preparing time

Table 1. *Demographic data on study subjects who underwent WLL*

Case	Age, yr	Sex	Symptoms*	Onset to WLL†, mo	DSS‡	Smoking Status	Occupational Dust Exposure	Complications
1	45	M	DOE, Occasional Cough	66	2	Ex-Smoker	No	Psoriasis, HT, DL
2	54	F	DOE	43	2	Never	No	HT, DL
3	67	M	Dyspnea, Cough, Hemosputum	10	5	Ex-Smoker	No	Postcerebral Infarction
4	34	M	Dyspnea	42	5	Current Smoker	No	None
5	53	F	Dyspnea, Cough	96	5	Never	No	SSS
6	46	M	None	30	1	Current Smoker	Yes	None
7	66	M	DOE	25	4	Never	No	DM
8	67	F	Dyspnea	36	5	Never	No	None
9	57	M	DOE	28	2	Never	No	None

*Symptoms were recognized as respiratory symptoms. †Onset: time when the 1st respiratory symptom emerged or time of finding an abnormal image that was compatible with pulmonary alveolar proteinosis (PAP). ‡Disease severity score (DSS): defined based on respiratory symptoms and arterial oxygen tension (PaO_2; see Ref. 3). DSS 1: no symptoms and $PaO_2 \geq 70$ mmHg. DSS 2: symptomatic and $PaO_2 \geq 70$ mmHg. DSS 3: 60 mmHg $\leq PaO_2 < 70$ mmHg. DSS 4: 50 mmHg $\leq PaO_2 < 60$ mmHg. DSS 5: $PaO_2 < 50$ mmHg. WLL, whole-lung lavage; DOE, dyspnea on exertion; HT, hypertension; DL, dyslipidemia; SSS, sick sinus syndrome; DM, diabetes mellitus.

ranged 10–225 s, 120–425 s, 52–225 s, and 0–96 s, respectively. In 11 of 17 lungs, the retaining time was designed to be 120 s, but it was variable with 132–425 s in 6 lungs. Time required for other stages varied remarkably as shown in Table 3.

The initial volume of instilled saline ranged within 600–2,300 ml (1,359 ± 435 ml). The initial discharged volume ranged from 150 to 1,282 ml (697 ± 341 ml), with percentage of recovery ranging from 24.3 to 71.4%. The mean volume of instilled saline from the second to the last lavage in each patient varied from 489 to 1,938 ml (893 ± 374 ml). In each cycle, 461–1,896 ml (859 ± 364 ml) of discharged fluid was recovered; the recovery percentage was relatively constant (89.7–100.3%). As a whole, the total volume of saline instilled into each lung was 9,900–28,200 ml, and the total volume of discharged lavage fluid was 8,910–27,000 ml, with total percentage of recovery of 93.4 ± 3.3 (82.1–95.9%).

Simulation of Protein Concentrations in the Drained Lavage Fluid

The theoretical concentrations of IgG, transferrin, albumin, and β_2- microglobulin in the drained lavage fluid were calculated at the end of the draining stage according to the equation described above and by using the procedures detailed in MATERIALS AND METHODS. The theoretical concentrations were plotted on a log scale against time after the beginning of WLL (Fig. 2). The plot for each patient was manually fitted with the protein concentration measured in the drained lavage fluid of each cycle by changing K_s and K_b. Plots for the theoretical concentrations of IgG, transferrin, albumin, and β_2-microglobulin coincide with the measurements (Fig. 2, *A–D*). Data for K_s and K_b are shown in Fig. 3. K_s values for IgG, transferrin, albumin, and β_2-microglobulin ($2.03 \times 10^{-7} \pm 0.902$, $1.95 \times 10^{-7} \pm 0.589$, $1.84 \times 10^{-7} \pm 0.564$, and $1.85 \times 10^{-7} \pm 0.658$, respectively) did not vary among patients (Fig. 3*A*). Importantly, there was no significant difference in K_s values among these four proteins, suggesting that transfer from the surfactant to lavage fluid was independent of molecular weight. However, there was relative variability in K_b among proteins, especially with β_2-microglobulin, which had a K_b that was two orders of magnitude higher than that of the other proteins. K_b values for IgG, transferrin, albumin, and β_2-microglobulin were $4.97 \times 10^{-10} \pm 4.166$, $5.61 \times 10^{-10} \pm 1.990$, $3.82 \times 10^{-10} \pm 1.661$, and $2.28 \times 10^{-8} \pm 0.773$, respectively (Fig. 3*B*). No differences in K_s or K_b values of each protein were found between left and right lungs (data not

Table 2. *Clinical parameters of patients*

	Arterial Blood Gas Analysis			Serum Biomarkers				Pulmonary Function Test			
Case	PaO_2, mmHg	$PaCO_2$, mmHg	A-aDO_2, mmHg	KL-6, IU/ml	SP-D, ng/ml	CEA, ng/ml	GM-Ab, μg/ml	%VC, %	FEV_1/FVC, %	FRC, liters	$\%DL_{CO}$, %
1	81.3	35.8	24.0	7611	963	6.9	6.8	85.8	82.7	2.51	60.5
2	75.6	39.4	25.1	32070	187	12.5	116.0	81.9	79.43	1.77	38.2
3	67.4*	35.5*	269.0*	46700	518	41.4	25.2	51.4	84.5	2.36	19.2
4	55.2*	38.4*	167.7*	26300	799	49.1	25.0	47.7	78.98	1.52	30.0
5	46.4	34.8	60.1	31093	422	19.8	35.7	47.4	98.1	1.41	ND†
6	72.3	38.8	29.2	8356	236	12.8	35.5	85.9	82.9	2.49	70.7
7	51.2	36.7	52.9	10969	407	73.3	6.7	87.5	109.4	1.71	70.8
8	46.2	38.2	55.1	15700	531	16.5	10.4	77.5	80.3	1.53	ND
9	75.3	39.6	24.9	7684	172	7.9	150.9	83.9	75.8	2.50	67.8

Normal Krebs von den Lungen-6 (KL-6), surfactant protein D (SP-D), carcinoembryonic antigen (CEA), and granulocyte/macrophage colony-stimulating factor autoantibody (GM-Ab) levels were within 500 IU/ml, 110 ng/ml, 5.0 ng/ml, 1.0 μg/ml, respectively. *Nasal oxygen supply. †Diffusing capacity of the lung for carbon monoxide (DL_{CO}) of case 5 was not detected because of low vital capacity (VC). ND, not done. A-aDO_2, alveolar-arterial oxygen difference that was measured; FEV_1, forced expiratory volume in 1 s; FVC, forced vital capacity; FRC, functional residual capacity.

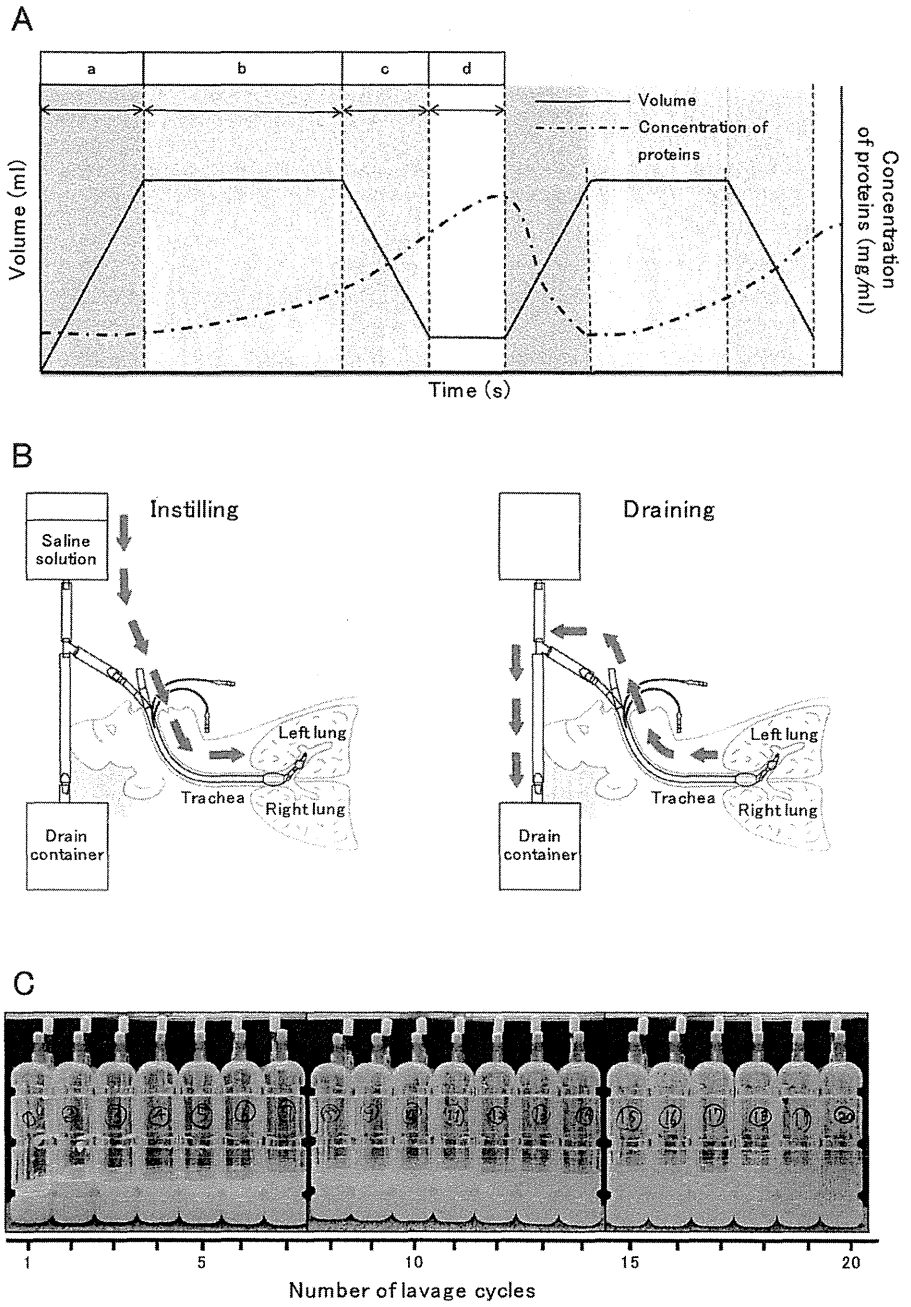

Fig. 1. *A*: conceptual schematic of the time course of the lavage fluid volume in the lung and the concentration of a protein during whole-lung lavage (WLL). Each lavage cycle involved 4 stages: instilling (*a*, from the beginning to the end of saline instillation), retaining (*b*, from the end of saline instillation until the beginning of drainage), draining (*c*, from the beginning to the end of drainage), and preparing (*d*, from the end of drainage to the beginning of the next saline instillation). *B*: schematic of the procedures for instilling (*left*) and draining (*right*) stages. ~0.5 to 2.0 l of saline solution from a bottle was instilled through an endotracheal tube into the lavage lung, retained for a few minutes, and then drained into a draining container. *C*: appearance of the drained fluid obtained from the first to the 20th lavage cycle.

shown). Thus the simulation data confirm the appropriateness of our mathematical model and indicate that the transfer kinetics of proteins into the drained fluid was time dependent.

Durable Effects of the Time on the Lavage Efficiency

To determine the durable effect of each lavage cycle on the slope for the decreasing concentration of each protein in the drained lavage fluid, we evaluated the change in slope of the theoretical curves by varying the duration of the retaining stage in silico. For this purpose, we used the initial data settings in case 4, i.e., the instilling volume of saline; the durations (s) of instillation, retaining, draining, and preparing; and the volume of drained lavage fluid in the first lavage cycle. We found that decreasing curves for the albumin concentration became steeper upon substitution of the shorter time (Fig. 4*A*).

Next, we proceeded to confirm the effects observed in the simulation by using measurements in case 1. We evaluated the rate of declining albumin concentration in the lavage aliquots from a patient who occasionally underwent WLL for the left lung with short-term cycles (120 s, 1–20 cycles) and for the right lung with long-term cycles (540 s, 4–11 cycles). As shown in Fig. 4*B*, the slope of decline for the left lung appeared